MOLECULAR AND CELLULAR BIOLOGY, Nov. 1997, p. 6223–6235 Vol. 17, No. 11
0270-7306/97/$04.00+0

Role of *UME6* in Transcriptional Regulation of a DNA Repair Gene in *Saccharomyces cerevisiae*

DOUGLAS H. SWEET,† YEUN KYU JANG, AND GWENDOLYN B. SANCAR*

Department of Biochemistry and Biophysics, School of Medicine, The University of North Carolina at Chapel Hill, Chapel Hill, North Carolina 27599-7260

Received 16 December 1996/Returned for modification 13 February 1997/Accepted 5 August 1997

In *Saccharomyces cerevisiae* UV radiation and a variety of chemical DNA-damaging agents induce the transcription of specific genes, including several involved in DNA repair. One of the best characterized of these genes is *PHR1*, which encodes the apoenzyme for DNA photolyase. Basal-level and damage-induced expression of *PHR1* require an upstream activation sequence, UAS_{PHR1}, which has homology with DRC elements found upstream of at least 19 other DNA repair and DNA metabolism genes in yeast. Here we report the identification of the *UME6* gene of *S. cerevisiae* as a regulator of UAS_{PHR1} activity. Multiple copies of *UME6* stimulate expression from UAS_{PHR1} and the intact *PHR1* gene. Surprisingly, the effect of deletion of *UME6* is growth phase dependent. In wild-type cells *PHR1* is induced in late exponential phase, concomitant with the initiation of glycogen accumulation that precedes the diauxic shift. Deletion of *UME6* abolishes this induction, decreases the steady-state concentration of photolyase molecules and *PHR1* mRNA, and increases the UV sensitivity of a *rad2* mutant. Despite the fact that UAS_{PHR1} does not contain the URS1 sequence, which has been previously implicated in *UME6*-mediated transcriptional regulation, we find that Ume6p binds to UAS_{PHR1} with an affinity and a specificity similar to those seen for a URS1 site. Similar binding is also seen for DRC elements from *RAD2*, *RAD7*, and *RAD53*, suggesting that *UME6* contributes to the regulated expression of a subset of damage-responsive genes in yeast.

Cells respond to environmental stress by altering growth and developmental programs to counteract the effects of the stress and to ensure the survival of the cell or organism. These changes reflect modulation of the specificity or activity of specific proteins as well as induction or repression of specific genes. The cellular response to UV-induced stress is one of the best characterized of these responses. In eukaryotes, UV radiation and other DNA-damaging agents activate cell cycle checkpoints and induce transcription of genes encoding proteins involved in DNA repair and damage tolerance. These processes are linked through one or more signal transduction pathways, the components of which have been most extensively characterized for *Saccharomyces cerevisiae*. In this organism UV damage-responsive checkpoints can be activated in G_1, S, or G_2 phase (reviewed in reference 41). While current evidence suggests that the damage-sensing components may differ (41), all three checkpoints, as well as the transcriptional response, require the protein kinases encoded by *MEC1* and *RAD53* (23, 41, 60). The Dun1 protein kinase, which functions downstream of Mec1 and Rad53, is also required for the transcriptional response of at least some damage-responsive genes but is not required for cell cycle arrest (41, 72). Recently another protein kinase, Hrr25, has been implicated in the transcriptional response (18); however, the relationship of this kinase to the Mec1-Rad53-Dun1 pathway remains undefined.

Identification of the transcriptional regulators that are the ultimate targets of the damage signal transduction pathway is crucial to understanding the mechanism of the damage response. While more than 20 damage-inducible genes have been described for *S. cerevisiae*, the transcription factors that regulate expression of these genes are largely unknown. The transcriptional activators Msn2 and Msn4, acting through the stress-response element (STRE), control a group of genes that respond to multiple stresses, including heat shock, osmotic stress, nitrogen starvation, and oxidative stress (including oxidative stress induced by agents that also damage DNA) (35, 49). However, the relevance of this induction to DNA damage and repair is not clear, because none of the STRE-regulated genes identified thus far play roles in DNA repair. The Swi4 and Swi6 transcription factors are required for induction of *RNR2* and *RNR3* (which encode subunits of ribonucleotide reductase) in response to methyl methanesulfonate or hydroxyurea; however, it is not known whether this reflects a direct interaction with an *RNR* promoter element(s), nor have the sequences required for Swi4/Swi6-mediated induction of the *RNR* genes been identified (18). The 5′ flanking regions of at least 19 DNA repair and metabolism genes contain similar sequence elements, known as DRC elements (47), and it has been reported that the single-stranded-DNA-binding protein replication protein A (RP-A) binds in vitro to oligonucleotides containing similar elements from *RAD1*, *RAD2*, *RAD4*, *RAD10*, *RAD16*, *RAD51*, *RNR2*, *RNR3*, *PHR1*, *DDR48*, *MGT*, and *MAG* (55). However, an in vivo role for RP-A in the transcriptional regulation of these genes has not been established.

In this communication we report the cloning and identification of a transcriptional regulator of the *S. cerevisiae* DNA repair gene *PHR1*. *PHR1* encodes the apoenzyme for the repair enzyme DNA photolyase. This enzyme catalyzes the light-dependent repair of cyclobutane-type pyrimidine dimers in DNA and stimulates "dark repair" of these lesions via a mechanism that requires an active nucleotide excision repair pathway (48). *PHR1* transcription is induced by a variety of DNA-

* Corresponding author. Mailing address: Department of Biochemistry and Biophysics, CB# 7260, University of North Carolina at Chapel Hill, Chapel Hill, NC 27599-7260. E-mail: gsancar.biochem@mhs.unc.edu.

† Present address: Laboratory of Pharmacology and Chemistry, National Institute of Environmental Health Sciences, Research Triangle Park, NC 27709.

TABLE 1. Oligonucleotides used in this study

Name	Sequence[a]	Sequence location (gene)[b]	Reference
ACTtop	5′-TCTATCGTCGGTCGACCAAGACAC-3′	405→429	
ACTbot	5′-ATGGAAGATGGAGGCAAAGC-3′	1282′→1261′	
pBRBAMcw	5′-TACTTGGAGCCACTATCGACTACGCGATCA-3′	3733→3762 (*tet*)	6
pBRBAMccw	5′-TAGGCGCCAGCAACCGCACCTGT-3′	3850′→3828′ (*tet*)	6
DUG6PCR1	5′-CCACTATCGACTACGAGATCTTGGCGACC-3′	3742→3770 (*tet*)	6
DUG6ccw	5′-TGCTCGTACCAGATCTGGTAGAAATTTGGCTTATCAGTACG-3′	2764′→2740′ (*UME6*)	59
RIUAStop	5′-AATTCTTTTCTTCCTCGTTTTTCGAGGAAGCAG-3′	−121→−93 (*PHR1*)	47
RIUASbot	5′-AATTCTGCTTCCTCGAAAAACGAGGAAGAAAAG-3′	−93′→−121′ (*PHR1*)	47
MIXUAS1	5′-GGGATAGTGCGACCGTAGTGCCTGCATG-3′		
MIXUAS2	5′-CAGGCACTACGGTCGCACTATCCC-3′		
MIXUAS1-EcoRI	5′-AATTCATAGTGCGACCGTAGTGCCTGG-3′		
MIXUAS2-EcoRI	5′-AATTCCAGGCACTACGGTCGCACTATG-3′		
P-PAL-Stop	5′-CTTTTCTTCCTCGTTTTTCGAGGAAGCAGTGCATG-3′	−121′→−93 (*PHR1*)	47
P-PAL-Sbot	5′-CACTGCTTCCTCGAAAAACGAGGAAGAAAAGTGCA-3′	−93′→−121′ (*PHR1*)	47
P-ΔCGA-Stop	5′-CTTTTCTTCCTTTTTGGAAGCAGTGCATG-3′		
P-ΔCGA-Sbot	5′-CACTGCTTCCAAAAAGGAAGAAAAGTGCA-3′		
P-mCGA-Stop	5′-CTTTTCTTCCACTTTTTACGTGGAAGCAGTGCATG-3′		
P-mCGA-Sbot	5′-CACTGCTTCCACGTAAAAAGTGGAAGAAAAGTGCA-3′		
P-mGAAG-Stop	5′-CTTTTTGCACTCGTTTTTCGACACAGCAGTGCATG-3′		
P-mGAAG-Sbot	5′-CACTGCTGTGTCGAAAAACGAGTGCAAAAAGTGCA-3′		
PHR347	5′-ATGTCATCACTGCAGATGATTGGAGAG-3′	347→373	46
PHR1266	5′-TGCTACAGGGTTATTCTCCCATT-3′	1266′→1244′	46
SPO13top	5′-AATTCGAAATAGCCGCCGACAAAAAGGAATTG-3′	−101→−76 (*SPO13*)	4
SPO13bot	5′-AATTCAATTCCTTTTTGTCGGCGGCTATTTCG-3′	−76′→−101′ (*SPO13*)	4
MAGURS2top	5′-AATTCTCTTTTCGGTGGCGATGAATG-3′	−180→−161 (*MAG*)	55, 68
MAGURS2bot	5′-AATTCATTCATCGCCACCGAAAAGAG-3′	−161′→−180′ (*MAG*)	55, 68
RAD2top	5′-AATTCGAACCTCCGTGGAGGCATTAAAAGGGAG-3′	−177→−149 (*RAD2*)	31
RAD2bot	5′-AATTCTCCCTTTTAATGCCTCCACGGAGGTTCG-3′	−149′→177′ (*RAD2*)	31
RAD7top	5′-AATTCTTATTTATGGAAGCAAAAATGGAATAAAG-3′	−129→−101 (*RAD7*)	43
RAD7bot	5′-AATTCTTTATTCCATTTTTGCTTCCATAAATAAG-3′	−101′→−129′ (*RAD7*)	43
RAD53top	5′-AATTCATCACCGTGGGTAGACTTGGAAATG-3′	−237→−211 (*RAD53*)	71
RAD53bot	5′-AATTCATTTCCAAGTCTACCCACGGTGATG-3′	−211′→−236′ (*RAD53*)	71

[a] Underlined bases were added to introduce restriction sites or complementary ends for cloning.
[b] Numbers refer to locations relative to the translational start site of the gene in the reference given. Primes indicate sequence on the noncoding strand.

damaging agents, including 254-nm radiation, methylmethane sulfonate, 4-nitroquinoline oxide, nitrosoguanidine, and *cis*-platin (24, 50), but is not induced by heat shock or photoreactivating light. Deletion and mutation analysis of *PHR1* 5′ flanking sequences has identified three regulatory elements that contribute to basal-level and induced expression: a 22-bp palindrome (URS_{PHR1}) that is the binding site for the damage-responsive repressor PRP, an upstream activation sequence (UAS_{PHR1}) comprised of two DRC elements arranged as an interrupted molecular palindrome, and a novel essential sequence (UES_{PHR1}) which antagonizes repressor binding or function (47, 51). UAS_{PHR1} is required for constitutive and high-level induced expression of *PHR1* but does not appear to be damage responsive, at least in the context of a heterologous promoter. To further characterize the transcriptional regulation of *PHR1*, we have carried out a screen for genes which, when present in multiple copies, enhance expression from UAS_{PHR1}. This screen has identified the transcriptional regulator *UME6* as a multicopy enhancer of *PHR1* activity. Deletion of *UME6* has demonstrable effects on expression of *PHR1* in the absence of DNA damage and on UV sensitivity and photoreactivation. Evidence that these effects are the result of direct interaction between UAS_{PHR1} and Ume6 protein (Ume6p) is presented. We also find that Ume6p binds specifically to DRC elements from *RAD2*, *RAD7*, and *RAD53*, suggesting that *UME6* may be a common regulator of a group of DNA repair genes.

MATERIALS AND METHODS

Oligonucleotides. The oligonucleotides used in this study are listed in Table 1.

Plasmids and plasmid constructions. Plasmid constructions and transformation of *Escherichia coli* were performed by standard techniques. Plasmid structures were confirmed by restriction endonuclease digestion patterns and, where indicated, by DNA sequence analysis. Plasmids pBM1501, pPAL, pRS415, pRS416, pGBS116, pMAL-*UME6*, YEp24, pHY14-2, and pHY16-2 and the Carlson-Botstein *Saccharomyces cerevisiae* genomic library have been described previously (3, 6, 11, 40, 47, 50, 54, 59). Plasmid pPRTCM was a gift from Howard Fried (University of North Carolina at Chapel Hill); it is a CEN plasmid carrying *TRP1* and the *TCM1-lacZ* fusion from pTCMZ2 (15).

Plasmids containing *HIS3* and *lacZ* reporter genes were generated as follows. Plasmid pBM1501 carries the *S. cerevisiae HIS3* gene, including the TATA box, but lacks a functional UAS (11). pGBS287 (Fig. 1) was constructed by ligating annealed DNA oligonucleotides RIUAStop and RIUASbot, which contain UAS_{PHR1}, into the *Eco*RI site upstream of *HIS3* in pBM1501, thereby placing expression of *HIS3* under the control of UAS_{PHR1}. The β-galactosidase reporter plasmid pGBS501 (Fig. 1) was produced by ligating a 4-kbp *Sma*I-*Sca*I fragment, containing the UAS_{PHR1}-*CYC1-lacZ* construct from pPAL (47) (Fig. 1), into *Nae*I-*Sma*I-digested pRS415. pGBS203, pGBS204, pGBS205, and pGBS206 are derivatives of pGBS501 and were constructed by ligation of various hybridized oligonucleotides into pGBS501 which had been digested with *Sph*I and *Pst*I. Each construction replaced the UAS_{PHR1} fragment and approximately 250 bp of vector sequence with either an intact or a mutated UAS_{PHR1} element. Oligonucleotides used in these constructions were P-ΔCGA-Stop and P-ΔCGA-Sbot for pGBS203, P-PAL-Stop and P-PAL-Sbot for pGBS204, P-mCGA-Stop and P-mCGA-Sbot for pGBS205, and P-mGAAG-Stop and P-mGAAG-Sbot for pGBS206. The presence and orientation of UAS_{PHR1} elements in each of the above-described plasmids were confirmed by DNA sequencing.

pGBS503 (Fig. 1) was isolated during our library screen and is a YEp24 derivative containing ~4.5 kbp of *S. cerevisiae* genomic DNA inserted at the unique *Bam*HI site (6). The insert contains unique *Sph*I and *Pvu*II sites. pGBS508 and pGBS510 (Fig. 2) are subclones derived from pGBS503 and were constructed as follows. pGBS503 was digested with *Sph*I, yielding 8.9- and 3.1-

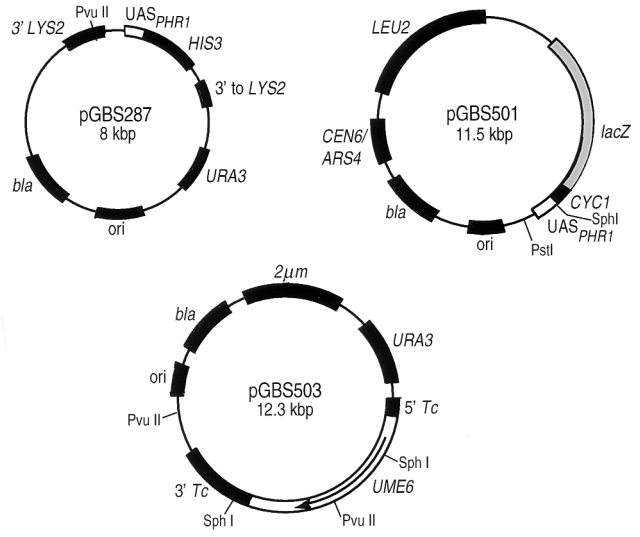

FIG. 1. Reporter plasmids used in this study. pGBS501 and pGBS503 are *S. cerevisiae-E. coli* shuttle vectors. pGBS287 is a yeast integrating plasmid with integration directed to a region 3′ to *LYS2*, as described in Materials and Methods. Open boxes indicate either UAS$_{PHR1}$ inserted upstream of the indicated reporter gene or the *S. cerevisiae* chromosomal insert carrying *UME6*, as labeled. The location of the *UME6* coding sequence and direction of transcription are indicated by the curved arrow. Gray box, *lacZ* coding sequences. Black boxes, relevant *E. coli* and *S. cerevisiae* genetic elements with names indicated.

kbp fragments. Self-ligation of the 8.9-kbp fragment yielded pGBS508, and ligation of the 3.1-kbp fragment into YEp24 digested with *Sph*I yielded pGBS510. To construct pGBS512 and pGBS514 (Fig. 2), pGBS503 was digested with *Pvu*II, yielding fragments of 8.7 and 3.2 kbp. Self-ligation of the 8.7-kbp fragment produced pGBS512, and ligation of the 3.2-kbp fragment into YEp24 digested with *Pvu*II produced pGBS514. PCR was used to amplify the *UME6* sequence from pGBS503 by using the primers DUG6PCR1 and DUG6ccw; the amplified fragment was digested with *Bgl*II and inserted into the *Bam*HI site of YEp24, yielding pGBS520 (Fig. 2). Insertion of a 4.2-kbp *Hin*dIII fragment, containing the entire yeast genomic insert from pGBS503, into *Hin*dIII-digested pUC19 yielded pGBS516. To construct the *UME6* knockout plasmid pGBS517, the *LEU2* gene in pRS415 was amplified by PCR with primers that added unique *Bss*HII and *Mlu*I sites immediately 5′ and 3′ to the gene. This fragment was

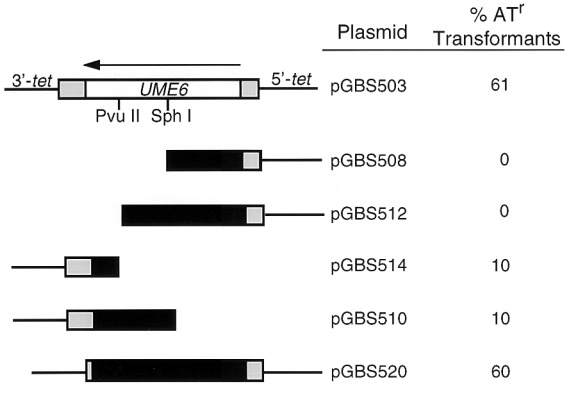

FIG. 2. Deletion analysis of the yeast genomic fragment carried by pGBS503. The genomic fragment carried by pGBS503 is shown as a box, with the limits of the *UME6* coding sequence and direction of transcription indicated. Gray boxes indicate yeast genomic sequences 5′ and 3′ to the *UME6* coding sequence. The extent of the genomic fragment remaining in each deletion construct is indicated by the black and gray boxes. The percentage of AT^r transformants was determined by transforming naive GBS242 with each plasmid and selecting separately for Ura$^+$ transformants and AT^r transformants. Control transformations with YEp24 yielded 4% AT^r transformants; this value has been subtracted from the values shown.

ligated into *Bss*HII-*Mlu*I-digested pGBS516, thereby replacing the 2.4-kbp *Bss*HII-*Mlu*I fragment of *UME6* (59) with *LEU2*.

Yeast culture. Yeast strains were routinely propagated at 30°C in yeast extract-peptone-adenine-dextrose (YPAD) or synthetic complete medium (SC) lacking Trp, Ura, His, or Leu as previously described (47). Library screen plates (SC lacking His, Leu, and Ura) also contained 3-amino-1,2,4-triazole (3AT) (Sigma Chemical Company) at a concentration of 20 mM. *ura3* mutants or strains that had lost *URA3*-containing plasmids were selected by growth on 5-fluoroorotic acid (American Biorganics) agar.

Yeast strains. All yeast strains used in this study are listed in Table 2. Integration of pGBS287 adjacent to the genomic *LYS2* gene of RE1007 was directed by cutting the plasmid at a unique *Pvu*II site within *LYS2* 3′ flanking sequences (11), yielding strain GBS149. Integration was confirmed by Southern analysis of genomic DNA, mitotic stability of the *URA3* marker under nonselective growth conditions, and growth of GBS149 on SC lacking His. Strain GBS153 is a derivative of GBS149 which lost the integrated *URA3* sequences via intrachromosomal homologous recombination between sequences 3′ to *LYS2* but retained the UAS$_{PHR1}$-*HIS3* reporter gene. The library screen strain GBS242 was constructed by transforming pGBS501 into GBS153. GBS783 is a derivative of GBS153 containing pRS415. GBS118 is isogenic to the previously described strain GBS117, in which the genomic *PHR1* locus has been replaced by a *PHR1-lacZ* fusion gene (50). 5-Fluoroorotic acid selection for spontaneous mutations inactivating *URA3* in GBS118 yielded GBS231. Strains GBS238 and GBS239 are independent isolates from a transformation of pGBS503 into GBS231. Strains GBS235 and GBS236 were obtained by curing GBS238 of pGBS503, and GBS237 was isolated by curing GBS239 of pGBS503. Strains GBS1001, GBS1002, GBS1003, GBS1061, GBS1063, GBS1330, GBS1333, GBS1336, GBS1339, GBS1351, GBS1353, GBS1358, and GBS1361 are transformed derivatives of yC105 (59) and contain the plasmids indicated in Table 2. Strain GBS1072, in which *UME6* is replaced by *LEU2*, was generated by transforming GBS77 with pGBS518 digested with *Bam*HI and *Hin*dIII.

UV survival. Late-log-phase cultures (A_{600} = 1.0; ~10^7 cells/ml) grown in liquid SC lacking Ura were harvested by centrifugation, washed in phosphate-buffered saline, suspended, and irradiated at 254 nm as previously described (48). Photoreactivation was carried out under the same conditions as 254-nm irradiation except that a BLB black lamp was used, the fluence rate was 0.9 J/m^2/s, and the photoreactivation period was limited to 5 min. Repair of pyrimidine dimers by photolyase nullifies the lethal effects of a portion of the UV dose. The dose decrement, ΔD, is defined as the difference between the UV doses with and without photoreactivation that yield the same surviving fraction (17). The number of pyrimidine dimers repaired was obtained by multiplying ΔD by the number of dimers introduced per haploid genome per joule per square meter, which has been estimated as 240 (65).

Glycogen determination. Samples (50 to 100 ml) were collected from log-phase cultures of GBS1001 and GBS1002 grown in SC lacking Ura. Cells were pelleted by centrifugation at 2,000 × *g* at 4°C for 10 min, washed once with ice-cold water, pelleted, suspended in 0.5 ml of 0.25 M Na_2CO_3, and stored at −70°C. Conversion of glycogen to glucose and assays of glucose concentration were performed as described by Francois et al. (12) and Skroch (56) with the following modifications: 5 ml of enzyme color reagent (Diagnostics Procedure 510; Sigma Chemical Company) was added to 0.5 ml of cleared lysate, and the mixture was incubated at 37°C for 30 min. Glucose concentrations were determined by A_{440} with reference to a glucose standard curve.

Library screen. A YEp24-based yeast genomic library (6), previously amplified once, was purified from *E. coli* and transformed into GBS242. Transformed cells were plated onto Hybond N filters (Amersham), overlaid onto plates containing SC lacking Leu and Ura, and incubated at 30°C for 18 to 24 h, at which time the filters were transferred to screen medium plates (SC lacking Leu, Ura, and His and containing 20 mM 3AT) and incubated for 7 more days. Prolonged incubation was necessary due to slow growth on the screen medium. After 7 days, the nylon filters were lifted, frozen in liquid nitrogen for 1 min, and placed on filter paper (Whatmann no. 1) soaked in β-galactosidase assay solution (5 ml of Z buffer [37], 39 mM β-mercaptoethanol, 334 μg of 5-bromo-4-chloro-3-indolyl-β-D-galactopyranoside per ml). The filters were incubated at 30°C for 2 to 4 h and examined for colonies that turned blue faster than similarly treated control colonies of GBS783 and GBS242. Four independent colonies from each positive clone were recovered and retested. Plasmids from clones that displayed a positive phenotype upon retesting were recovered by transformation into *E. coli*; plasmid DNA was isolated and used to transform naive GBS242, looking for correlation between survival on screen medium and survival on SC lacking Leu and Ura.

Southern and Northern analyses. Primers pBRBAMcw and pBRBAMccw were used in PCR to obtain full-length copies of the yeast genomic inserts from pGBS503 and pGBS504. PCRs were by standard techniques with the addition of Taq Extender (as specified by the manufacturer [Stratagene]) to aid amplification of the long template. PCR products were purified (PCR Cleanup Kit; Promega), labeled (ECL Direct Nucleic Acid Labeling System; Amersham), and used as probes in Southern analysis of *Eco*RI-digested DNAs from pGBS503 to pGBS507.

For Northern analysis of *PHR1* mRNA, 50 μg of total RNA, extracted from early-log-phase (A_{600} = 0.1 to 0.2) or late-log-phase (A_{600} = 1.2 to 1.5) cultures of GBS1001 and GBS1002, was electrophoresed through 1.2% agarose gels containing 2.2 M formaldehyde and transferred to GeneScreen Plus nylon mem-

TABLE 2. *S. cerevisiae* strains used in this study

Strain	Genotype[a]	Source or reference
GBS77	α *rad2 leu2-3,112 ura3-52*	50
GBS118	**a** *PHR1-lacZ-URA3 leu2-3,112 trp1 ura3-52*	50
GBS149	α *can1-100 his3-11,15 leu2-3,112 trp1-1 ura3-52 LYS2::*UAS_{PHR1}*-HIS3-URA3*	This work
GBS153	α *can1-100 his3-11,15 leu2-3,112 trp1-1 ura3-52 LYS2::*UAS_{PHR1}*-HIS3*	This work
GBS231	**a** *PHR1-lacZ-ura3 leu2-3,112 trp1 ura3-52*	This work
GBS235	GBS238 cured of pGBS503	This work
GBS236	GBS238 cured of pGBS503	This work
GBS237	GBS239 cured of pGBS503	This work
GBS238	Isogenic to GBS231 (pGBS503)	This work
GBS239	Isogenic to GBS231 (pGBS503)	This work
GBS242	Isogenic to GBS153 (pGBS501)	This work
GBS783	Isogenic to GBS153 (pRS415)	This work
GBS1001	Isogenic to yC105 (pGBS501 and YEp24)	This work
GBS1002	Isogenic to yC105 (pGBS501 and pHY14-2)	This work
GBS1003	Isogenic to yC105 (pGBS501 and pHY16-2)	This work
GBS1061	Isogenic to yC105 (pPRTCM and YEp24)	This work
GBS1063	Isogenic to yC105 (pPRTCM and HY16-2)	This work
GBS1072	α Δ*ume6::LEU2 rad2 leu2-3,112 ura3-52*	This work
GBS1330	Isogenic to yC105 (pGBS204 and pHY14-2)	This work
GBS1333	Isogenic to yC105 (pGBS203 and pHY14-2)	This work
GBS1336	Isogenic to yC105 (pGBS205 and pHY14-2)	This work
GBS1339	Isogenic to yC105 (pGBS206 and pHY14-2)	This work
GBS1351	Isogenic to yC105 (pGBS203 and YEp24)	This work
GBS1353	Isogenic to yC105 (pGBS204 and YEp24)	This work
GBS1358	Isogenic to yC105 (pGBS205 and YEp24)	This work
GBS1361	Isogenic to yC105 (pGBS206 and YEp24)	This work
RE1007	α *can1-100 his3-11,15 leu2-3,112 trp1-1 ura3-52*	M. Johnston
yC105	**a** *ade2-1 ade6 can1-100 his3-11,15 leu2-3,112 trp1-1 ura3-1 ume6-D1*	59

[a] Plasmids carried by strains are indicated in parentheses.

branes as previously described (20). Probes for *PHR1* and *ACT1* mRNAs were obtained by PCR amplification of specific regions of these genes from S288C genomic DNA by using oligonucleotides PHR347, PHR1266, ACT1top, and ACT1bot (Table 1). The purified fragments were labeled by the random hexamer priming method with [^{32}P]dCTP and were hybridized to the Northern blots. Hybridized counts per minute were quantitated with a Molecular Dynamics PhosphoImager.

Liquid β-galactosidase assays. Plasmid-containing strains were grown in liquid medium, and 1.0- to 1.5-ml samples were collected in triplicate, pelleted by centrifugation at 12,000 × *g* for 10 min at 4°C, washed with 1.5 ml of Z buffer, and repelleted. The Z buffer was removed, and cell pellets were frozen at −80°C. For strains GBS235 to GBS240, in which the *lacZ* reporter construct is integrated into the genome, 50-ml samples were collected. For the assay, cell pellets were thawed at room temperature for 3 to 5 min, suspended in 100 μl of assay reagent (Z buffer containing 43 mM β-mercaptoethanol, 0.2 mM phenylmethylsulfonyl fluoride, 10 μg of apoprotinin per ml, 10 μg of soybean trypsin inhibitor per ml, 4 μg of leupeptin per ml, and 520 μg of Zymolyase T100 per ml), and incubated at 35°C for 1.5 to 2 h. At the end of the incubation period, the cells were vortexed vigorously for 45 s and immediately placed on ice. Forty microliters of the cell lysate was added to 160 μl of reaction cocktail (12 mM β-mercaptoethanol, 50 μl of 100 μg of 4-methylumbelliferyl-β-D-galactoside per ml, 25 mM Tris [pH 7.5], 125 mM NaCl, 2 mM $MgCl_2$) and placed immediately at 37°C. After a 30-min incubation, the reaction was stopped by addition of 50 μl of ice-cold 25% trichloroacetic acid. The tubes were chilled on ice for at least 10 min and then spun in a microcentrifuge at full speed for 4 min immediately prior to fluorescence determination. One hundred microliters of sample supernatant was added to 1.9 ml of glycine carbonate buffer (133 mM glycine, 83 mM Na_2CO_3, pH 10.7), and the fluorescence of the product, 4-methylumbelliferon, was determined in a TKO 100 minifluorometer (Hoefer) (excitation wavelength = 365 nm; emission wavelength = 460 nm). One unit of β-galactosidase activity is defined as 1 pmol of 4-methylumbelliferon produced per ml of culture per A_{600} unit of cells in a 30-min assay. Each strain was tested on at least two different occasions.

Ume6 protein expression and purification. Maltose binding protein (MBP)-Ume6 fusion protein was obtained by isopropylthio-β-D-galactoside induction (0.3 mM for 2 h) of pMAL-Ume6 in *E. coli* CAG456 grown at 30°C (59), followed by cell lysis and maltose affinity chromatography according to the manufacturer's instructions (Protein Fusion and Purification System; New England Biolabs). The MBP-Ume6 protein obtained in this manner was estimated to be ~30% pure by sodium dodecyl sulfate-polyacrylamide gel electrophoresis followed by staining with Coomassie blue. The major contaminant migrated with MBP.

Electrophoretic mobility shift assays. Probes for electrophoretic mobility shift assays were made by hybridizing the complementary oligonucleotide pairs RIUAStop-RIUASbot, MIXUAS1-MIXUAS2, MIXUAS1-EcoRI–MIXUAS2-EcoRI, SPO13top-SPO13bot, MAGURS2top-MAGURS2bot, RAD2top-RAD2bot, RAD7top-RAD7bot, and RAD53top-RAD53bot. Five micrograms of each oligonucleotide was mixed in a final volume of 100 μl of 200 mM NaCl, heated to 95°C for 5 min, and then allowed to slowly cool to room temperature. Probes were labeled with [α-^{32}P]dATP (800 Ci/mmol; Amersham) by using Klenow enzyme. The labeled probes were purified (NucTrap columns; Stratagene), followed by extraction with phenol-chloroform and ethanol precipitation. Recoveries and specific activities of labeled probes were determined by electrophoresis of aliquots on 6% nondenaturing polyacrylamide gels followed by quantitation of radioactivity with an Ambis Radioanalytic Imaging System. Protein binding reactions were carried out for 15 min at room temperature in 20-μl volumes containing binding buffer (4 mM Tris [pH 8.0], 4 mM $MgCl_2$, 40 mM NaCl), 10 μg of apoprotinin per ml, 10 μg of soybean trypsin inhibitor per ml, 4 μg of leupeptin per ml, 10% glycerol, 100 μg of bovine serum albumin per ml, 5 mM dithiothreitol, and 5 mM phenylmethylsulfonyl fluoride; the MBP-Ume6 protein, probe, and competitor were at the concentrations indicated in the figure legends. For MBP control reactions, 260 nM purified MBP (a gift from Aziz Sancar) was used. Bound and free probe were separated on 6% nondenaturing polyacrylamide gels electrophoresed at 150 V for 2.75 h. Gels were dried, and radioactivity was quantified with an Ambis Radioanalytic Imaging System. Bound material was designated as all counts in material migrating slower than the free probe band after subtraction of background counts in the "bound" region of the MBP control lane (generally <10% of total counts).

RESULTS

Cloning of *UME6* as a multicopy enhancer of UAS_{PHR1} activity. UAS_{PHR1} retains its function in the context of heterologous promoters (47). This permitted us to devise a selection scheme for genes that, when present in multiple copies, enhance expression from UAS_{PHR1}. The strain used to screen for such genes, GBS242, contained two reporter genes: an integrated chimeric gene, UAS_{PHR1}*-HIS3*, in which *HIS3* expression is driven from UAS_{PHR1}, and a UAS_{PHR1}*-CYC1-lacZ* gene carried on the *CEN* plasmid pGBS501. Unlike the parental

TABLE 3. Effect of *UME6* and *rim16-2* on expression from *PHR1*, UAS_{PHR1}, and *TCM1*

Strain	Relevant chromosomal genotype	Relevant plasmid genotype (copy no.)	Reporter (location)	β-Galactosidase activity (U)[a] in:	
				Early log phase ($A_{600} \leq 0.4$)	Late log phase ($A_{600} \geq 1.0$)
GBS238	*UME6*	*UME6* (multicopy)	*PHR1-lacZ* (chromosome)	54 ± 6	ND[b]
GBS235	*UME6*	No plasmid	*PHR1-lacZ* (chromosome)	10 ± 1	ND
GBS236	*UME6*	No plasmid	*PHR1-lacZ* (chromosome)	12 ± 1	ND
GBS239	*UME6*	*UME6* (multicopy)	*PHR1-lacZ* (chromosome)	37 ± 5	ND
GBS237	*UME6*	No plasmid	*PHR1-lacZ* (chromosome)	11 ± 2	ND
GBS1001	Δ*ume6*	YEp24 (multicopy)	UAS_{PHR1}-*lacZ* (CEN plasmid)	840 ± 170	850 ± 120
GBS1002	Δ*ume6*	*UME6* (1–2)	UAS_{PHR1}-*lacZ* (CEN plasmid)	1,660 ± 320	5,630 ± 1,450
GBS1003	Δ*ume6*	*rim16-12* (1–2)	UAS_{PHR1}-*lacZ* (CEN plasmid)	1,250 ± 260	4,050 ± 660
GBS1061	Δ*ume6*	YEp24 (multicopy)	*TCM1-lacZ* (CEN plasmid)	344,600 ± 41,000	39,700 ± 3,200
GBS1063	Δ*ume6*	*UME6* (1–2)	*TCM1-lacZ* (CEN plasmid)	244,300 ± 21,300	42,711 ± 2,700

[a] Means ± standard deviations.
[b] ND, not determined.

strain R1007, GBS242 grew in the absence of exogenous histidine, confirming that UAS_{PHR1} functions in the context of the *HIS3* promoter. GBS242 was transformed with an *S. cerevisiae* genomic library constructed in the multicopy plasmid YEp24 (6), and Ura^+ transformants carrying genes that enhanced expression from UAS_{PHR1} were selected by virtue of their ability to grow on 20 mM 3AT, a competitive inhibitor of the *HIS3* gene product. Ura^+ $3AT^r$ clones were then tested for enhanced expression of the UAS_{PHR1}-*CYC1-lacZ* reporter. Thirty-two clones positive in both tests were initially identified among 17,700 Ura^+ transformants. Following plasmid rescue in *E. coli* and transformation into naive GBS242, library plasmids from five clones (pGBS503 to pGBS507) retained the ability to confer the $3AT^r$ phenotype in >60% of Ura^+ transformants. (The frequency of $3AT^r$ clones presumably reflects a threshold of *HIS3* expression reached in only a subpopulation of transformants carrying multiple copies of the plasmid.) Restriction analysis of these plasmids indicated that each contained an ~4.5-kbp insert of yeast genomic DNA that contained two *Eco*RI sites separated by 2.4 kbp. Southern analysis of *Eco*RI-digested plasmid DNA revealed that the genomic inserts from pGBS503 and pGBS504 hybridized strongly to each of the five plasmids but not to YEp24 alone (data not shown). We concluded that all five plasmids contain the same genomic insert and limited further characterization to the library clone pGBS503.

Using primers PBRBAMcw and PBRBAMccw, which hybridize, respectively, to *tet* sequences upstream and downstream of the cloned DNA fragment, we determined the nucleotide sequence of ~250 bp from each end of the genomic insert and compared these to *S. cerevisiae* sequences in the GenBank and *S. cerevisiae* genomic databases. A 100% match was obtained between the 3′ 160 bp primed from PBRBAMcw and sequences −841 to −681 from the published 5′ flanking region of the bifunctional transcriptional regulator *UME6* (59). Likewise, a 100% match was found to 65 bp primed from PBRBAMCCW and sequences within the 3′ end of YDR206W, an open reading frame of unknown function that resides adjacent to the 3′ end of *UME6* on chromosome IV (7). The presence of the entire *UME6* gene was confirmed by digestion of pGBS503 with a battery of restriction enzymes that span the complete *UME6* coding region as well as 841 bp of 5′ flanking region and 522 bp of 3′ flanking sequences (59). To confirm that *UME6* is responsible for enhanced expression from UAS_{PHR1}, we introduced subclones of pGBS503 that contained various portions of the genomic insert into naive GBS242. As can be seen in Fig. 2, only plasmid pGBS520, which contains the entire *UME6* coding region and 5′ flanking sequence and 258 bp of 3′ flanking sequence, conferred a level of 3AT resistance comparable to that seen with the library plasmid pGBS503.

Multiple copies of *UME6* enhance expression of *PHR1* in its normal chromosomal context. Expression of *PHR1* is governed by three upstream regulatory elements which lie in close proximity within the *PHR1* 5′ regulatory region (47). An important question is whether by removing UAS_{PHR1} from its native context, we altered its regulatory properties either by eliminating interactions between proteins bound to contiguous promoter elements or by fortuitously introducing a new regulatory site during construction of the reporter genes. To address this question, we introduced pGBS503 (*UME6*) into strain GBS231, in which the chromosomal copy of *PHR1* has been replaced by an integrated *PHR1-lacZ* translational fusion (50). β-Galactosidase activities in two transformed isolates (GBS238 and GBS239) was compared to those seen in isogenic derivatives which had lost pGBS503 (GBS235, GBS236, and GBS237). As can be seen in Table 3, multiple copies of *UME6* stimulated expression of the *PHR1-lacZ* reporter three- to fivefold in early-log-phase cultures.

Effects of a *UME6* deletion on vegetative expression of *PHR1*. Is the effect of *UME6* on *PHR1* expression limited to the nonphysiological condition in which *UME6* is overexpressed? To address this question, we compared expression driven by UAS_{PHR1} in log-phase vegetative cells from strain GBS1001, which carries a deletion of the entire *UME6* coding sequence, with that seen in GBS1002, which carries *UME6* on a CEN vector present in one or two copies per cell. *PHR1* expression is influenced by the stage of the growth cycle (25). Early in log phase in glucose-containing media, *PHR1* is expressed at a constant level, while in late log phase expression increases five- to sevenfold. This behavior is recapitulated in strains carrying the UAS_{PHR1}-*lacZ* reporter plasmid pGBS501 (Fig. 3). The onset of enhanced *PHR1* expression appears to coincide with the onset of glycogen accumulation (Fig. 3B) that immediately precedes the switch from fermentative to oxidative metabolism known as the diauxic shift (27). Deletion of *UME6* altered two features of this expression pattern. First, as can be seen in Table 3 and Fig. 3B (compare strains GBS1001 and GBS1002),

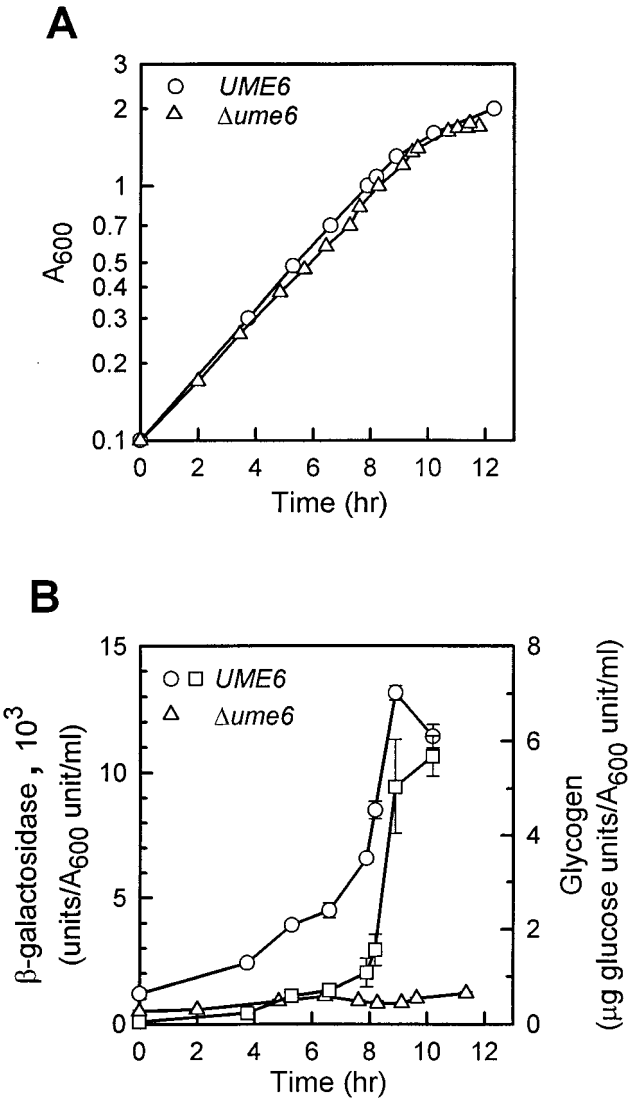

FIG. 3. Effect of a deletion of *UME6* on cell growth and expression from UAS_{PHR1}. Cultures of strains GBS1001 (Δ*ume6*) and GBS1002 (*UME6*) growing in liquid media were monitored for growth and expression from UAS_{PHR1}-*lacZ* as described in Materials and Methods. (A) Growth of the cultures monitored by A_{600}. (B) Expression from UAS_{PHR1}-*lacZ* (○ and △) and glycogen accumulation in strain GBS1002 (□). Error bars indicate standard deviations from two to four independent β-galactosidase or glycogen assays.

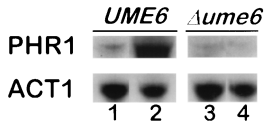

FIG. 4. Northern analysis of *PHR1* mRNA levels in the presence or absence of *UME6*. Total RNA was extracted from early-log-phase cultures (lanes 1 and 3) and late-log-phase cultures (lanes 2 and 4) of GBS1001 (Δ*ume6*) and GBS1002 (*UME6*), separated, and probed as described in Materials and Methods. Hybridization to mRNA from the *ACT1* gene served as an internal loading control. Autoradiograms of the electrophoretic mobility shift assay gels were scanned with a UMAX UC840 flat-bed scanner; the image was imported into Adobe Photoshop for labeling and output.

levels of the fusion protein in early log phase were reduced by approximately 50% in the Δ*ume6* background. While this effect is small, it is entirely reproducible and has been seen in each of four independent isolates of each genotype. Second, deletion of *UME6* abolished the enhanced accumulation of the fusion protein in late log phase. To determine whether these changes reflect events at the intact *PHR1* promoter in its normal chromosomal location, we performed Northern analysis of *PHR1* mRNA from early-log-phase and late-log-phase cultures of GBS1001 and GBS1002. As we have reported previously and is apparent in Fig. 4, the steady-state concentration of *PHR1* mRNA in early-log-phase cells is extremely low (50), and this level is diminished approximately 40% in the absence of a functional *UME6* gene (compare lanes 1 and 3). Consistent with the studies using the *lacZ* reporter plasmid, the steady-state concentration of *PHR1* mRNA increased dramatically (approximately 15-fold) in late-log-phase cells, and this increase was dependent upon the presence of an active *UME6* gene (compare lanes 2 and 4 of Fig. 4). Two observations indicate that these effects are specific for *PHR1* rather than the consequence of a general pleiotropic effect on gene expression: (i) accumulation of most individual mRNA species decreases or is unchanged in late log phase (reviewed in reference 67; also see the *ACT1* control in Fig. 4), and (ii) as can be seen in Table 3 (compare GBS1061 and GBS1063), deletion of *UME6* did not alter the expression pattern exhibited by the housekeeping gene *TCM1*, which encodes the ribosomal protein L3. Thus, *UME6* plays a specific, dual role in *PHR1* expression. *UME6* enhances basal-level expression of *PHR1* during the fermentative stage of cell growth, and *UME6* is required for *PHR1* induction immediately preceding the diauxic shift.

Although it was initially identified as a repressor of vegetative expression of early meiotic genes (58), *UME6* also plays a role in the meiotic activation of some of these genes (3, 45). Activation is achieved through interaction between Ume6p and the transcriptional activator Ime1p at a *cis*-acting regulatory site known as URS1. URS1 is thought to be the binding site for Ume6p or a complex containing Ume6p (39, 45, 57, 59). In **a**/α diploids, starvation for nitrogen and glucose leads to activation of Ime1p, recruitment of Ime1p to the URS1 site through interaction with Ume6p, and transcriptional activation of the early meiotic genes (3, 39, 45). Although *IME1* mRNA is present at very low levels during vegetative growth (22), the fact that *IME1* expression is regulated in response to cyclic AMP (cAMP) levels (36) suggested to us that Ime1p might contribute to the enhanced expression of *PHR1* seen during the diauxic shift. We tested this hypothesis by using a *UME6* allele known as *rim16-12*; the protein encoded by *rim16-12* retains the ability to repress early meiotic genes during vegetative growth but is defective in Ime1p-mediated transcriptional activation (3). As can be seen in Table 3, strain GBS1003, which carries a deletion of *UME6* and the *rim16-12* allele on a CEN plasmid, supported a 3.2-fold induction of the reporter in late log phase, compared to a 3.4-fold induction with the wild-type *UME6* gene. These results suggest that interaction between Ume6p and Ime1p is not required for induction of UAS_{PHR1} at the diauxic shift in haploid vegetative cells.

Ume6p binds specifically to UAS_{PHR1}. Genetic evidence indicates that the bifunctional transcriptional regulatory sequence URS1 (consensus sequence, AGCCGCCGA [30]) is a site of *UME6* action (39, 42, 45, 57, 59, 61), and both full-length Ume6p and an MBP-Ume6p fusion protein containing amino acids 560 to 836 bind to URS1 in vitro (1, 59). The sequence of UAS_{PHR1}, TTTTCTTCCTCGTTTTTCGAGGAAGCAGT, does not contain a good match to the URS1 consensus (see Fig. 6B), suggesting that the effect of *UME6* on *PHR1* expression might be mediated through another *UME6*-regulated pro-

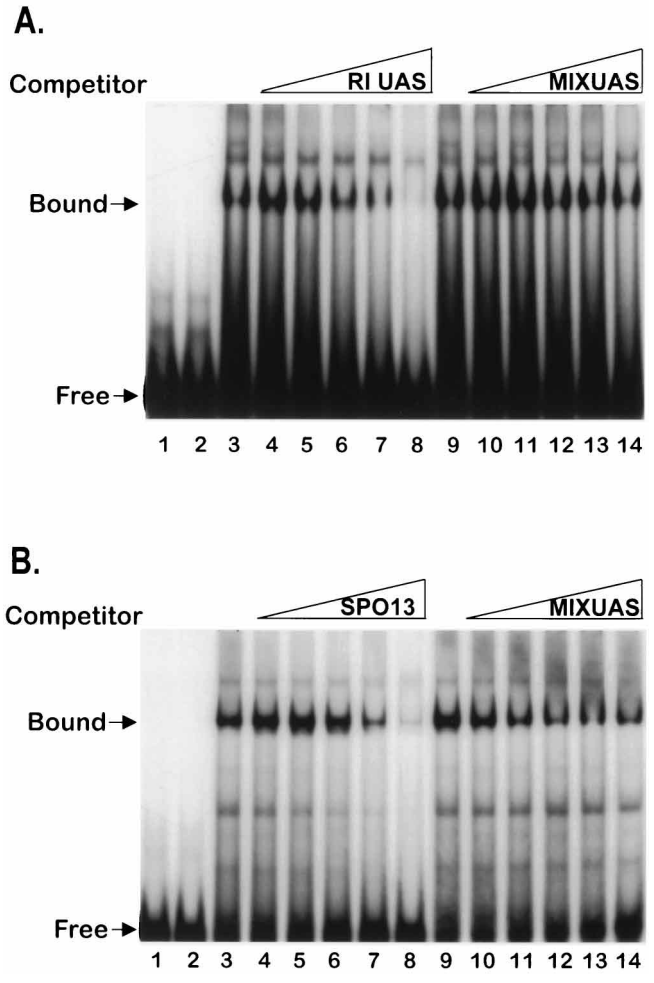

FIG. 5. Electrophoretic mobility shift assays demonstrating the affinity and specificity of MBP-Ume6p binding to UAS_{PHR1} and *SPO13* URS1. Assays were performed as described in Materials and Methods with 10 nM labeled RIUAS (A) or SPO13 URS1 (B) oligonucleotide, 80 nM MBP-Ume6p or purified MBP, and various concentrations of either homologous or heterologous unlabeled competitor oligonucleotide. Lanes: 1, labeled oligonucleotide only; 2, labeled oligonucleotide plus purified MBP; 3 to 8, labeled oligonucleotide plus MBP-Ume6p and 0, 10, 20, 50, 150, or 500 nM, respectively, unlabeled homologous (RIUAS or SPO13 URS1) oligonucleotide; 9 to 14, labeled oligonucleotide plus MBP-Ume6p and 0, 10, 20, 50, 150, or 500 nM, respectively, unlabeled heterologous (MIXUAS) oligonucleotide. Scanning of the autoradiogram and image production were as described in the legend to Fig. 4.

tein rather than through physical interaction of Ume6p with UAS_{PHR1}. To test this possibility, we utilized the electrophoretic mobility shift assay to assess the binding of the MBP-Ume6p fusion protein constructed by Stritch and coworkers (59) to UAS_{PHR1}.

The MBP-Ume6p fusion protein formed a major complex and a minor complex with the UAS_{PHR1} oligonucleotide RIUAS (Fig. 5A). Binding of Ume6p in the major complex was specific as judged by the difference in response to increasing concentrations of unlabeled homologous versus heterologous (MIXUAS) competitor. A 10-fold molar excess of unlabeled RIUAS reduced formation of the major labeled complex by 80%, while the same concentration of unlabeled MIXUAS reduced complex formation by only 20% (Fig. 5A, lanes 7 and 13). In contrast, formation of the minor complex was largely unaffected by addition of up to a 50-fold molar excess of homologous or nonspecific competitor (Fig. 5A, lanes 8 and 14), suggesting that this complex reflects nonspecific interaction with MBP-Ume6p.

In view of the absence of a URS1 consensus sequence in UAS_{PHR1}, it was of interest to compare the affinity of Ume6p for UAS_{PHR1} to that for an extensively characterized *UME6*-responsive regulatory sequence containing URS1. The *SPO13* URS1 element was chosen for this comparison (59). MBP-Ume6p displayed a slightly higher affinity for the *SPO13* URS1 oligonucleotide than for the RIUAS oligonucleotide (compare lanes 3 in Fig. 5A and B). At equimolar substrate and MBP-Ume6p concentrations approximately 55% of the *SPO13* URS1 oligonucleotide was bound, compared to 30% of the RIUAS oligonucleotide. A 10-fold excess of homologous competitor reduced MBP-Ume6p binding to labeled *SPO13* URS1 by 60%, while the same concentration of nonspecific competitor reduced binding by 20%. Based on these data and direct titration experiments (data not shown), we estimate that the equilibrium association constants (K_As) for MBP-Ume6p binding to the oligonucleotides are 2.0 ($\pm$0.4) $\times$ 10^7 M^{-1} for SPO13 URS1, 1.29 ($\pm$0.14) $\times$ 10^7 M^{-1} for RIUAS, and 1.08 ($\pm$0.4) $\times$ 10^6 M^{-1} for MIXUAS. Thus, the affinities and specificities of MBP-Ume6p binding to UAS_{PHR1} and to *SPO13* URS1 are similar.

Ume6 binds to other DRC elements from yeast. The 5′ flanking regions of at least 19 yeast genes involved in DNA repair and damage tolerance contain a sequence element known as DRC which has the consensus sequence G/CGA/TGGA/CRRNANA/T (47). UAS_{PHR1} consists of an interrupted palindrome comprised of two DRC elements flanking five T's. DRC elements are also found upstream of the damage-responsive genes *RAD2*, *RAD7*, *RAD16*, *RAD23*, *RAD53* (also known as *SPK1* and *MEC2*), and *MAG*. In the cases of *RAD2* (53), *RAD23* (44a), *RAD53* (cited in reference 68), *MAG* (68), and *PHR1* (47), regions containing the DRC elements have been shown to be involved in regulated expression of the genes. Does Ume6p recognize DRC elements from genes other than *PHR1*? As can be seen in Fig. 6A, oligonucleotides containing single DRC elements from *MAG* URS2, *RAD2*, *RAD7*, and *RAD53* form complexes with MBP-Ume6p. Quantitation of the fraction of Ume6p-bound probe revealed that the extent of complex formation for each of these DRC elements was similar to that seen with UAS_{PHR1} and *SPO13* URS1: RIUAS, 29% (Fig. 6A, lane 2); *SPO13* URS1, 40% (lane 6); *MAG* URS2, 22% (lane 10); *RAD2*, 27% (lane 15); *RAD7*, 35% (lane 19); and *RAD53*, 26% (lane 24). Furthermore, the responses of DRC elements from *RAD2*, *RAD7*, and *RAD53* to homologous and heterologous competitors paralleled those seen with RIUAS and *SPO13* URS1. The competition results shown in Fig. 6 are presented quantitatively in Table 4, from which it can be seen that a 3-fold excess of homologous competitor and a 15-fold excess of nonspecific competitor (MIXUAS) reduced binding to approximately similar extents for SPO13 URS1 and the DRC elements from UAS_{PHR1}, *RAD2*, *RAD7*, and *RAD53*. The DRC element from *MAG* URS2 was exceptional in that a threefold excess of homologous or heterologous competitor reduced binding to similar extents, suggesting that MBP-Ume6p does not discriminate well between *MAG* URS2 and the nonspecific competitor. This is surprising considering that *MAG* URS2 is the best match to the URS1 consensus among the elements tested (Fig. 6B).

The number of DNA binding sites on Ume6p has not been characterized. Thus, the binding of MBP-Ume6p to UAS_{PHR1} and *SPO13* URS1 could occur at different, distinct sites on the protein. To address this question, we examined the ability of *SPO13* URS1 and the DRC elements to compete for binding

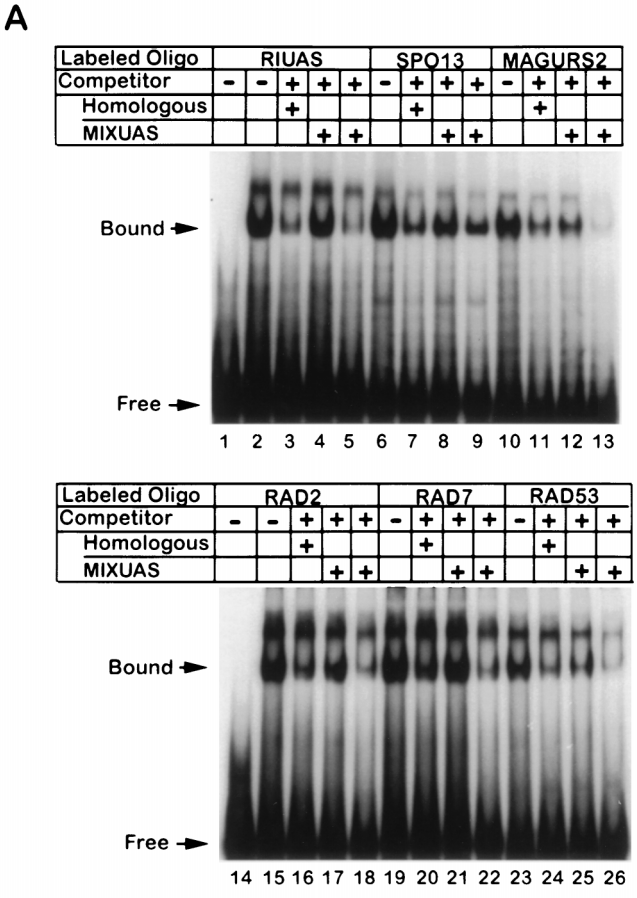

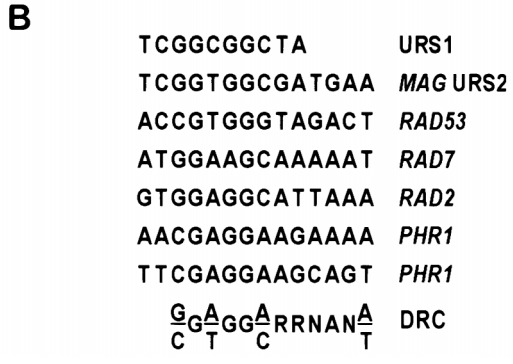

FIG. 6. (A) Electrophoretic mobility shift assays demonstrating the affinity and specificity of MBP-Ume6p for oligonucleotides containing DRC elements from *PHR1*, *SPO13*, *MAG*, *RAD2*, *RAD7*, and *RAD53*. Assays were performed as described in the legend to Fig. 5. Labeled oligonucleotides (oligo) were present at 80 nM and were as indicated. Lanes 1 and 14, purified MBP present at 260 nM. All other lanes contain MBP-Ume6p at 80 nM. Lanes 3, 7, 11, 16, 20, and 24, homologous unlabeled competitor at 240 nM; lanes 4, 8, 12, 17, 21, and 25, MIXUAS competitor at 240 nM; lanes 5, 9, 13, 18, 22, and 26, MIXUAS competitor at 1200 nM. Scanning of the autoradiogram and image production were as described in the legend to Fig. 4. (B) Alignment of the DRC sequences present in the oligonucleotide probes and comparison to the URS1 and DRC consensus sequences.

of MBP-Ume6p to UAS_{PHR1}. As can be seen in Fig. 7, the *SPO13* URS1 oligonucleotide competed efficiently with UAS_{PHR1} oligonucleotide for MBP-Ume6p binding. New complexes, which might reflect simultaneous binding of the two different oligonucleotides, were not observed. Consistent with the K_As reported above, *SPO13* URS1 and UAS_{PHR1} were similarly effective as competitors for Ume6p binding. Similar results were obtained when DRC elements from *RAD2*, *RAD7*, and *RAD53* were used as competitors (Fig. 7). As expected from the results obtained in the direct binding experiments, *MAG* URS2 competed significantly less well than the other regulatory elements despite the fact that it has 92% sequence identity with the DRC consensus sequence (Fig. 6B). It may be significant that *MAG* URS2 contains a G at position 10 of the DRC homology region, while all other DRC elements possess an A at this position.

TABLE 4. Competition of Ume6p-DNA complexes with homologous and MIXUAS oligonucleotides

Labeled probe (80 nM)	Fraction of bound counts remaining with the following competitor[a]:		
	Homologous (240 nM)	MIXUAS	
		240 nM	1,200 nM
RIUAS	0.20	0.64	0.22
SPO13	0.42	0.68	0.46
MAGURS2	0.39	0.50	0.12
RAD2	0.27	0.78	0.33
RAD7	0.36	0.77	0.27
RAD53	0.21	0.67	0.12

[a] Relative to bound counts in the absence of competitor.

Mutations in UAS_{PHR1} reduce Ume6p binding and *UME6*-dependent activation. If the in vitro binding of Ume6p reflects a physiologically significant interaction, then mutations in UAS_{PHR1} that reduce Ume6p binding might also be expected to reduce expression of the reporter in vivo. As an initial test of this hypothesis, we constructed plasmids in which all of the CGA elements in UAS_{PHR1} had been either deleted or mutated, as well as a plasmid in which the two GAAG elements that form part of the conserved core of the DRC elements were mutated. The CGA elements were targeted because they correspond to the CGPu general consensus for sites bound by

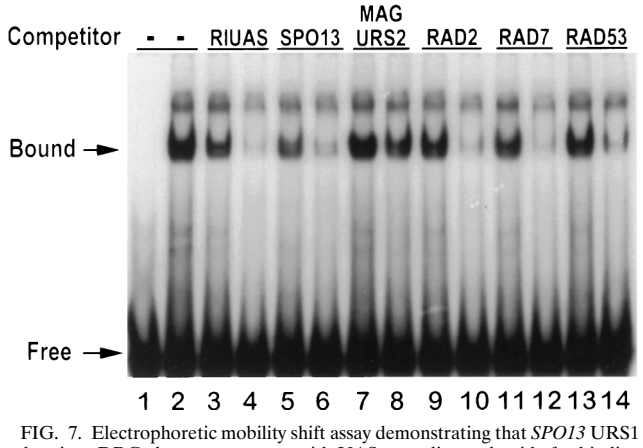

FIG. 7. Electrophoretic mobility shift assay demonstrating that *SPO13* URS1 and various DRC elements compete with UAS_{PHR1} oligonucleotide for binding of MBP-Ume6p. Assays were performed as described in Materials and Methods with RIUAS oligonucleotide at 80 nM as the labeled substrate. Lane 1, 260 nM purified MBP. All other lanes contain 80 nM MBP-UME6p. Lane 2, RIUAS and MBP-Ume6p only; lanes 3, 5, 7, 9, 11, and 13, 120 nM indicated competitor oligonucleotide; lanes 4, 6, 8, 10, 12, and 14, 560 nM indicated competitor oligonucleotide. Scanning of the autoradiogram and image production were as described in the legend to Fig. 4.

TABLE 5. Effect of mutations in UAS_{PHR1} on expression in *UME6* and Δ*ume6* backgrounds

UAS_{PHR1}[a]	Sequence[b]	K_A (10^7)	Strain	Genotype	β-Galactosidase activity (U)[c]		Induction ratio[d]
					$A_{600} < 0.25$	$A_{600} > 1.0$	
Intact	5′CTTTTCTTCCTCGTTTTTCGAGGAAGCAGT3′	1.4	GBS1330	*UME6*	2,400 (190)	13,800 (500)	5.8
	3′GAAAAGAAGGAGCAAAAAGCTCCTTCGTCA5′		GBS1353	Δ*ume6*	850 (170)	780 (130)	1.0
ΔCGA	5′CTTTTCTTCC---TTTTT---GGAAGCAGT3′	0.4	GBS1333	*UME6*	4,500 (140)	14,700 (1,500)	3.3
	3′GAAAAGAAGG---AAAAA---CCTTCGTCA5′		GBS1351	Δ*ume6*	1,800 (230)	2,400 (330)	1.3
mCGA	5′CTTTTCTTCCACTTTTTACGTGGAAGCAGT3′	0.8	GBS1336	*UME6*	2,790 (190)	7,300 (310)	2.6
	3′GAAAAGAAGGTGAAAAATGCACCTTCGTCA5′		GBS1358	Δ*ume6*	900 (180)	900 (90)	1.0
mGAAG	5′CTTTTTGCACTCGTTTTTCGACACAGCAGT3′	1.3	GBS1339	*UME6*	16,800 (1,500)	24,000 (2,500)	1.4
	3′GAAAAACGTGAGCAAAAAGCTGTGTCGTCA5′		GBS1361	Δ*ume6*	16,500 (1,800)	16,800 (2,300)	1.0

[a] m, mutant.
[b] Deletions are indicated by dashes; base replacements are underlined.
[c] Averages of three independent determinations with standard deviations shown in parentheses.
[d] β-Galactosidase units at an A_{600} of >1.0 divided by units at an A_{600} of <0.25.

fungal zinc binuclear cluster proteins (9). We chose to change multiple copies of the elements simultaneously because previous studies indicated that deletion or mutation of a single CGA or GAAG element had only a marginal effect on expression (47). Mutation of the three CGA elements reduced Ume6p binding in vitro by 40% as measured in binding competition assays, while deletion of the elements reduced binding by 70% (Table 5). In contrast, mutation of the GAAG elements had no effect on Ume6p binding. Due to the high nonspecific binding of Ume6p, complete elimination of the sequences specifically recognized by Ume6p is expected to decrease binding by no more than 90 to 95% in our in vitro assays. Therefore, the results suggest that the CGA sequences (or portions thereof) comprise a portion of the Ume6p recognition sequence. In vivo expression studies revealed that in the presence of *UME6*, both deletion and mutation of the CGA elements reduced the induction ratio (i.e., the level of expression in late log phase relative to that in early log phase) approximately twofold compared to that with the intact UAS; however, neither of these elements reduced basal-level expression. (Deletion of the CGA elements led to approximately twofold-greater basal-level expression. This increase is probably due to a nonspecific "spacing effect," since it was seen in six independent transformants [data not shown] and in both the presence and absence of *UME6*.) Deletion of *UME6* further reduced basal-level and induced expression from both constructs containing altered CGA elements. These results are consistent with either of two interpretations: (i) interaction of Ume6p with UAS_{PHR1} is mediated both through DNA contacts and through interaction with one or more additional proteins bound to the UAS, or (ii) *UME6* regulates expression from UAS_{PHR1} via two mechanisms, only one of which involves direct interaction between Ume6p and the UAS.

Mutation of the GAAG elements had unexpected effects: in the presence of *UME6*, basal-level expression increased fivefold and the induction ratio decreased to 25% of that seen with the intact UAS. Inactivation of *UME6* did not substantially affect expression from this mutant GAAG UAS. We believe that the results obtained with the mutant GAAG UAS are due to the fortuitous introduction of a new, Ume6-insensitive activator binding site. An alternative explanation is that the GAAG elements bind a repressor the activity of which is negatively regulated by *UME6*; however, this would not explain the correlation between decreased Ume6p binding and decreased induction observed when the CGA elements are modified.

Effect of a *UME6* deletion on UV sensitivity and photoreactivation. The results presented above indicate that *UME6* enhances expression of *PHR1* and may also contribute to the regulated expression of other DRC-containing genes. According to this model, a *ume6* deletion strain would be expected to exhibit reduced photoreactivation and perhaps also reduced survival in the absence of photoreactivation (dark survival). The UV survival data shown in Fig. 8 for late-log-phase GBS77 (*UME6*) and its isogenic derivative GBS1072 (Δ*ume6*) confirm this prediction. At all UV fluences tested, the absence of a functional *UME6* gene resulted in increased UV sensitivity (Fig. 8A). To determine the effect on photoreactivation, cells irradiated at various 254-nm fluences were exposed to a limiting fluence of photoreactivating light for 5 min. At all UV fluences of ≥ 2 J/m^2, GBS1072 (Δ*ume6*) displayed reduced dimer photorepair compared to GBS77 (*UME6*), consistent with a reduction in the steady-state concentration of active photolyase molecules (Fig. 8). From the data shown in Fig. 8A and similar experiments, we estimate that at 4 J/m^2, ΔD is 1.5 J/m^2 for GBS77 and 0.9 J/m^2 for GBS1072, which corresponds to photoreactivation of 360 dimers in the former strain and 240 dimers in the latter strain. This is a much smaller change in photoreactivation than might be predicted from the β-galactosidase data shown in Fig. 3. Several factors contribute to this difference: (i) it is clear from the slopes of the curves in Fig. 8B that substrate saturation was not reached, and this would lead to underestimation of the number of photolyase molecules; (ii) the β-galactosidase experiments measure the activity of UAS_{PHR1} in the absence of other regulatory elements which may attenuate the response of the intact *PHR1* promoter; and (iii) at low β-galactosidase concentrations a small increase in the concentration of monomers may produce a large increase in the number of active tetramers. The difference in photoreactivation produced by deletion of *ume6* is significant in light of previous studies which have shown that the number of photolyase molecules per cell is approximately twofold greater in stationary-phase *S. cerevisiae* cells than in log-phase cells (69). Our results indicate that a significant portion of this increase is *UME6* dependent.

DISCUSSION

The results reported in this study indicate that *UME6* is a positive regulator of *PHR1* transcription which acts through UAS_{PHR1}. Several lines of evidence support this conclusion. Multiple copies of *UME6* enhance expression from both UAS_{PHR1} and the intact *PHR1* promoter in its normal chromosomal context. Deletion of *UME6* abolishes induction from UAS_{PHR1} and from the intact promoter in late log phase. An MBP-Ume6p fusion protein containing the Ume6p DNA binding domain displays sequence-specific binding to UAS_{PHR1},

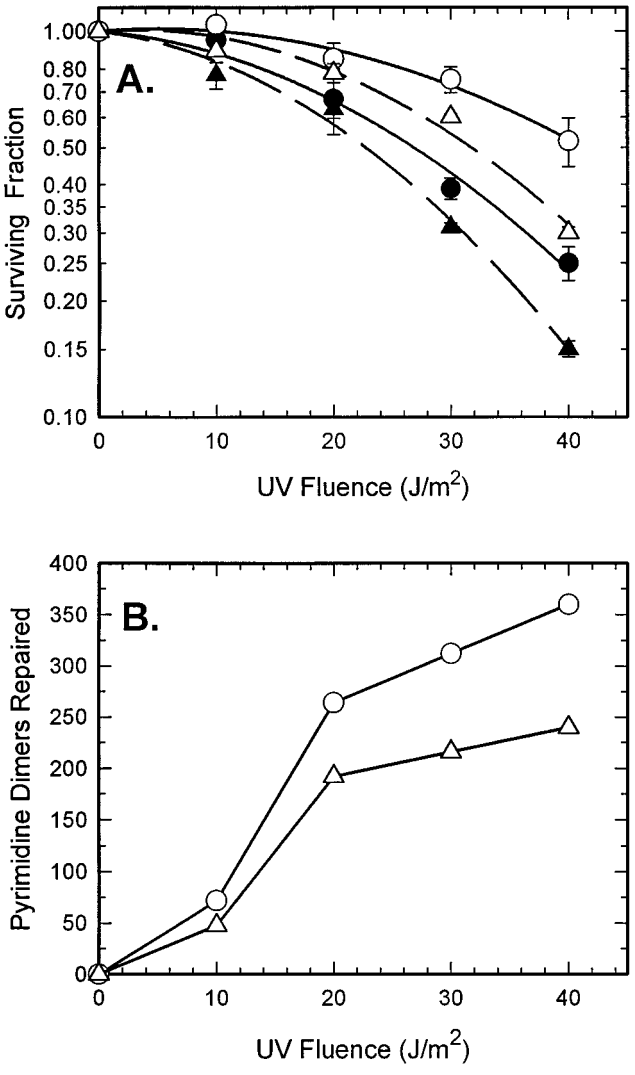

FIG. 8. UV survival and pyrimidine dimer repair in strains GBS77 (*UME6*) (circles) and GBS1072 (Δ*ume6*) (triangles). The strains were cultured, exposed to 254-nm radiation, and subsequently incubated in the dark either without (closed symbols) or with (open symbols) a 5-min period of photoreactivation as described in Materials and Methods. (A) Survival curves. (B) Number of pyrimidine dimers repaired during the 5-min photoreactivation period, calculated as described in Materials and Methods.

and alterations in the UAS that reduce Ume6p binding reduce expression in vivo. The most parsimonious explanation for these observations is that Ume6p exerts its effects in vivo by binding directly to UAS_{PHR1}. We wish to emphasize that *UME6* is not required for basal-level expression of *PHR1* in early log phase but rather enhances basal-level expression. This is indicated by the observation that deletion of *UME6* reduces expression from UAS_{PHR1} by no more than 70% during early-log-phase growth, and the same low level of UAS activity is maintained during later stages of growth in the absence of functional Ume6p. Thus, there must be additional proteins that bind to and activate UAS_{PHR1}. Given the small size of this region (29 bp), it is likely that Ume6p interacts with them.

Ume6p is a 91-kDa transcriptional regulator that contains a Zn_2Cys_6 binuclear cluster (1, 59) and is thus formally similar to other fungal binuclear transcriptional regulatory proteins, such as Gal4p, Ppr1p, and Hap1p (33, 34, 44). These proteins generally bind as homodimers to CGPu sequences arranged as molecular palindromes, direct repeats, or everted repeats, with the spacing between elements of the recognition sequence determined by a spacer region immediately following the binuclear cluster (reviewed in references 34 and 70). The spacer region is in turn followed by leucine-rich heptads which form the dimerization interface. Ume6p is an atypical member of this class in that it lacks the linker domain and leucine-rich dimerization domain and appears to bind DNA as a monomer (1). Circular dichroism studies indicate that in solution Ume6p has little stable secondary structure outside the helices immediately surrounding the binuclear zinc cluster, suggesting that interactions with other transcriptional regulatory proteins may control Ume6p folding (1). This may be similar to the situation recently reported for the Cdk inhibitor p21, which is largely disordered in solution but becomes highly ordered upon association with cyclin-Cdk complexes (26). Conformational flexibility may be directly relevant to the diversity of Ume6p function implied by our results.

UME6 regulates expression of a diverse group of genes involved in numerous metabolic pathways, including most of the early meiotic genes, *HSP82*, *INO1*, *FOX3*, and *CAR1* (10, 19, 39, 61). Deletion of *UME6* increases transcription of each of these genes during vegetative growth; thus, *UME6* formally functions as a repressor in these promoter contexts. These observations are in marked contrast to the role of *UME6* as an activator of *PHR1* expression during vegetative growth. Our results eliminate *IME1*, the *UME6*-dependent transcriptional activator of early meiotic genes (3, 45), as a required participant in activation of the UAS. However, our observation that mutations that strongly affect Ume6p binding in vitro have much smaller effects on expression in vivo are consistent with a role for protein-protein interactions in recruitment of Ume6p to the UAS. Sequence context differences have been proposed to explain differential requirements for Sin3p in Ume6p-mediated repression. Ume6p recruits the transcriptional corepressors Sin3 and Rpd3 to the *IME2* and *INO1* URS1 elements (21); however, URS1 elements from *TRK2* and *CAR1*, when placed in the context of the *CYC1* promoter, do not require Sin3 to mediate repression (42, 66). Perhaps sequence-induced changes in Ume6p structure play a role in determining interacting partners, as has been shown for Oct-1 (8, 38), or reveal an activation domain, as proposed for Mcm1p (63).

The URS1 element has the consensus sequence TAGCCG CCGA, and purified Ume6p protects the repeated CCG sequences from DNase I digestion (1). UAS_{PHR1} does not contain a good match to either the URS1 sequence or the CCG motif, yet Ume6p binds UAS_{PHR1} with an affinity and a specificity similar to those for the URS1 site in *SPO13*. Our results strongly suggest that a related sequence, CGA, which matches the general consensus CGPu for fungal zinc binuclear cluster proteins (9), forms a part of the Ume6p binding site in UAS_{PHR1}. We have not explored the sequence requirements for Ume6p binding to any of the other DRC-containing elements tested here; however, it is clear that Ume6p must recognize sequences in addition to CGA and CCG, because the RAD7 oligonucleotide used in these studies does not contain either sequence but is strongly bound by Ume6p. The crystal structures and solution structures of the zinc binuclear cluster proteins Gal4p, Ppr1p, and Lac9p indicate that the zinc cluster is usually compact and quite rigid (14, 33, 34). Nevertheless, this structure is sufficiently flexible to permit Hap1p to bind to both CGG and CGC triplets in the *CYC1* and *CYC7* promot-

ers, respectively (70). Our results suggest similar flexibility in Ume6p binding site selection.

The specificity of Ume6p binding is quite low for a sequence-specific DNA binding protein. We find that the equilibrium association constant (K_A) for interaction of MBP-Ume6p with $URS1_{SPO13}$ is only about 20-fold greater than that for a nonspecific oligonucleotide competitor of the same length. It is unlikely that this is an artifact introduced by use of a truncated fusion protein, because MBP alone does not bind the oligonucleotide with measurable affinity (this study), and the observed K_A for the fusion protein is only about fourfold lower than that reported for the interaction of full-length Ume6p with $URS1_{SPO13}$ (1). While estimates of nonspecific binding for full-length Ume6p have not been reported, a close examination of Fig. 6 in reference 1 suggests that at physiological salt concentrations the ratio of specific to nonspecific binding is within an order of magnitude of the value reported here. This low discrimination ratio predicts that in vivo, Ume6p could not efficiently find its cognate binding sites amid an excess of nonspecific binding sites. Possibly Ume6p is targeted to its binding sites in vivo via interactions with proteins that confer increased (and perhaps in some cases altered) binding specificity. The following circumstantial evidence suggests that RP-A may be such a Ume6p-interacting protein. (i) *UME6* is required for repression at $URS1_{CAR1}$, and RP-A, either purified or in crude extracts, binds specifically to this site (28, 29, 42). Comparable results have been reported for a URS1 site in the *FOX3* promoter (10). (ii) Crude extracts from Δ*ume6* strains display some differences in the pattern of $URS1_{CAR1}$–RP-A complexes (42). Similar changes have in the spectrum of complexes formed on the $URS1_{SPO13}$ have been noted, although the direct involvement of RP-A has not been demonstrated (59). (iii) RP-A binds to sequences from the 5′ regulatory regions of at least 12 yeast genes involved in DNA repair and DNA metabolism, including UAS_{PHR1} (55).

The *UME6*-dependent regulation of *PHR1* expression in response to growth cycle stage provides a mechanistic basis for earlier observations (69) that the number of active photolyase molecules is approximately twofold greater in stationary-phase cells than in log-phase cells. Induction of *PHR1* in late log phase coincides with the onset of glycogen accumulation that immediately precedes the switch from fermentative to oxidative carbon metabolism. The precise regulatory circuitry controlling this metabolic change, known as the diauxic shift, remains to be elucidated; however, it is clear that transcriptional and posttranslational processes are involved and that these processes are regulated, at least in part, through the *RAS*/cAMP/A-kinase and *SNF1* signal transduction pathways (5, 16, 64). Our results indicate that *UME6* directly links *PHR1* expression to the nutritional status of the cell. The level of *UME6* mRNA does not vary with nutritional status or during sporulation (59), and it is presumed that the same is true for Ume6p. Thus, the *UME6*-dependent activation of UAS_{PHR1} probably depends upon modification of Ume6p or other proteins at the UAS. A mechanism is immediately suggested by the fact that Ume6p contains four consensus sites for phosphorylation by cAMP-dependent protein kinase (59).

The potential regulation of *PHR1* by cAMP levels is reminiscent of the regulation of certain multistress-responsive genes in yeast and mammals. In *S. cerevisiae*, transcription of the multistress response genes *UBI4*, *CTT1*, *SSA3*, *HSP12*, and *TPS2* is negatively regulated by cAMP levels via a common STRE that is the binding site for the transcriptional activator Msn2p (2, 35, 49). In fission yeast the multistress response pathway is controlled by a different transcription factor, Atf1, that in vitro binds specifically to ATF/CRE sites that confer cAMP responsiveness (52, 62). Furthermore, like *UME6*, $atf1^+$ regulates the expression of a meiosis-specific transcription regulator (52, 57). Despite these similarities, the response of *PHR1* to UV and to nutritional status is clearly different from the general stress response. Unlike components of the multistress response, *PHR1* is not induced by heat shock (50), and there is not a match to the STRE or ATF/CRE consensus sequence within UAS_{PHR1}. A further difference pertains to the integration of the nutritional and UV responses. In the *PHR1* promoter, the nutritional response is conferred by UAS_{PHR1}-Ume6p, whereas the response to UV and other DNA-damaging agents is controlled primarily through an upstream repressor element and the damage-responsive repressor Prp (47, 51). In contrast, Msn2 and Atf1 are required for both the UV response and the nutritional response of the multistress response genes (32, 35, 49).

Understanding the mechanism through which *UME6* mediates induction of *PHR1* will likely require elucidation of the roles of the *RAS*/A-kinase and *SNF1* signal transduction pathways in this process as well as identification of proteins that interact with Ume6p at UAS_{PHR1}. In addition, the role of *UME6* in regulating expression of other DNA repair genes remains to be definitively addressed. It may be significant that the majority of damage-responsive genes in yeast are also induced early in meiosis (see reference 13 and references therein), at approximately the same time as the known *UME6*-dependent early meiotic genes (39). Finally, our results indicate that both the sequences recognized by Ume6p and the physiological consequences of Ume6p binding are more diverse than has been previously recognized.

ACKNOWLEDGMENTS

We thank Mark Johnson, Aaron Mitchell, Rochelle Esposito, Randy Strich, Michelle Sterber, and Howard Fried for providing plasmids and strains, Kelly Tatchell for helpful discussion, and Robert Ferris and Amy Wilson for excellent technical assistance.

This work was supported by grant GM35123 from the Public Health Service, Institute of General Medical Sciences.

REFERENCES

1. **Anderson, S. F., C. M. Steber, R. E. Esposito, and J. E. Coleman.** 1995. UME6, a negative regulator of meiosis in *Saccharomyces cerevisiae*, contains a C-terminal Zn_2Cys_6 binuclear cluster that binds the URS1 DNA sequence in a zinc-dependent manner. Protein Sci. **4:**1832–1843.
2. **Belazzi, T., A. Wagner, R. Wieser, M. Schanz, G. Adam, A. Hartig, and H. Ruis.** 1991. Negative regulation of transcription of the *Saccharomyces cerevisiae* catalase T (*CTT1*) gene by cAMP is mediated by a positive control element. EMBO J. **10:**585–592.
3. **Bowdish, K. S., H. E. Yuan, and A. P. Mitchell.** 1995. Positive control of yeast meiotic genes by the negative regulator *UME6*. Mol. Cell. Biol. **15:**2955–2961.
4. **Buckingham, L. E., H.-T. Wang, R. T. Elder, R. M. McCarroll, M. R. Slater, and R. E. Esposito.** 1990. Nucleotide sequence and promoter analysis of *SPO13*, a meiosis-specific gene of *Saccharomyces cerevisiae*. Proc. Natl. Acad. Sci. USA **87:**9406–9410.
5. **Cameron, S., L. Levin, M. Zoller, and M. Wigler.** 1988. cAMP-independent control of sporulation, glycogen metabolism, and heat shock resistance in *S. cerevisiae*. Cell **53:**555–566.
6. **Carlson, M., and D. Botstein.** 1982. Two differentially regulated mRNAs with different 5′ ends encode secreted and intracellular forms of yeast invertase. Cell **28:**145–154.
7. **Cherry, J. M., C. Adler, C. Ball, S. Dwight, S. Chervitz, G. Juvik, G. Wang, and D. Botstein.** 1996. Saccharomyces genome database. http://genome-www.stanford.edu/Saccharomyces/SacchDB9.10.96. 4.5.B12.
8. **Cleary, M. A., and W. Herr.** 1995. Mechanisms for flexibility in DNA sequence recognition and VP16-induced complex formation by the Oct-1 POU domain. Mol. Cell. Biol. **15:**2090–2100.
9. **De Rijcke, M., S. Seneca, B. Punyammalee, N. Glansdorff, and M. Crabeel.** 1992. Characterization of the DNA target site for the yeast ARGR regulatory complex, a sequence able to mediate repression or induction by arginine. Mol. Cell. Biol. **12:**68–81.
10. **Einerhand, A. W. C., W. Kos, W. C. Smart, A. J. Kal, H. F. Tabak, and T. G.**

Cooper. 1995. The upstream region of the *FOX3* gene encoding peroxisomal 3-oxoacyl-coenzyme A thiolase in *Saccharomyces cerevisiae* contains ABF1- and replication protein A-binding sites that participate in its regulation by glucose repression. Mol. Cell. Biol. **15:**3405–3414.
11. **Flick, J. S., and M. Johnston.** 1990. Two systems of glucose repression of the *GAL1* promoter in *Saccharomyces cerevisiae*. Mol. Cell. Biol. **10:**4757–4769.
12. **Francois, J., P. Eraso, and C. Gancedo.** 1987. Changes in the concentration of cAMP, fructose 2,6-bisphosphate and related metabolites and enzymes in *Saccharomyces cerevisiae* during growth on glucose. Eur. J. Biochem. **164:** 369–373.
13. **Friedberg, E. C., G. C. Walker, and W. Siede.** 1995. DNA repair and mutagenesis, p. 595–631. ASM Press, Washington, D.C.
14. **Gardner, K. H., S. F. Anderson, and J. E. Coleman.** 1995. Solution structure of the *Kluyveromyces lactis* LAC9 Cd_2Cys_6 DNA-binding domain. Nat. Struct. Biol. **2:**898–905.
15. **Hamil, K. G., H. G. Nam, and H. M. Fried.** 1988. Constitutive transcription of yeast ribosomal protein gene *TCM1* is promoted by uncommon *cis*- and *trans*-acting elements. Mol. Cell. Biol. **8:**4328–4341.
16. **Hardy, T. A., D. Huang, and P. J. Roach.** 1996. Interactions between cAMP-dependent and *SNF1* protein kinases in the control of glycogen accumulation in *Saccharomyces cerevisiae*. J. Biol. Chem. **269:**27907–27913.
17. **Harm, W., H. Harm, and C. S. Rupert.** 1968. Analysis of photoenzymatic repair of UV lesions in DNA by single light flashes. II. *In vivo* studies with *Escherichia coli* and bacteriophage. Mutat. Res. **6:**371–385.
18. **Ho, Y., S. Mason, R. Kobayashi, M. Hoekstra, and B. Andrews.** 1997. Role of the casein kinase I isoform, Hrr25, and the cell cycle-regulatory transcription factor, SBF, in the transcriptional response to DNA damage in *Saccharomyces cerevisiae*. Proc. Natl. Acad. Sci. USA **94:**581–586.
19. **Jackson, J. C., and J. M. Lopes.** 1996. The yeast *UME6* gene is required for both negative and positive transcriptional regulation of phospholipid biosynthetic gene expression. Nucleic Acids Res. **24:**1322–1329.
20. **Jang, Y. K., Y. H. Jin, M. J. Kim, R. H. Seong, S. H. Hong, and S. D. Park.** 1995. A simple and efficient method for the isolation of total RNA from the fission yeast *Schizosaccharomyces pombe*. Biochem. Mol. Biol. Int. **37:**339–344.
21. **Kadosh, D., and K. Struhl.** 1997. Repression by Ume6 involves recruitment of a complex containing Sin3 corepressor and Rpd3 histone deacetylase to target promoters. Cell **89:**365–371.
22. **Kassir, Y., D. Granot, and G. Simchen.** 1988. *IME1*, a positive regulator gene of meiosis in *Saccharomyces cerevisiae*. Cell **52:**853–862.
23. **Kiser, G. L., and T. A. Weinert.** 1996. Distinct roles of yeast *MEC* and *RAD* checkpoint genes in transcriptional induction after DNA damage and implications for function. Mol. Biol. Cell **7:**703–718.
24. **Knight, J. L., and G. B. Sancar.** 1997. Unpublished observations.
25. **Kraus, B., and G. B. Sancar.** 1997. Unpublished observations.
26. **Kriwacki, R. W., L. Hengst, L. Tennant, S. I. Reed, and P. E. Wright.** 1996. Structural studies of $p21^{Waf1/Cip1/Sdi1}$ in the free and Cdk2-bound state: conformational disorder mediates binding diversity. Proc. Natl. Acad. Sci. USA **93:**11504–11509.
27. **Lillie, S. H., and J. R. Pringle.** 1980. Reserve carbohydrate metabolism in *Saccharomyces cerevisiae*: responses to nutrient limitation. J. Bacteriol. **143:** 1384–1394.
28. **Luche, R. M., W. C. Smart, and T. G. Cooper.** 1992. Purification of the heteromeric protein binding to the URS1 transcriptional repression site in *Saccharomyces cerevisiae*. Proc. Natl. Acad. Sci. USA **89:**7412–7416.
29. **Luche, R. M., W. C. Smart, T. Marion, M. Tillman, R. Sumrada, and T. G. Cooper.** 1993. *Saccharomyces cerevisiae* BUF protein binds to sequences participating in DNA replication in addition to those mediating transcriptional repression (*URS1*) and activation. Mol. Cell. Biol. **13:**5749–5761.
30. **Luche, R. M., R. Sumrada, and T. G. Cooper.** 1990. A *cis*-acting element present in multiple genes serves as a repressor protein binding site for the yeast *CAR1* gene. Mol. Cell. Biol. **10:**3884–3895.
31. **Madura, K., and S. Prakash.** 1986. Nucleotide sequence, transcript mapping, and regulation of the *RAD2* gene of *Saccharomyces cerevisiae*. J. Bacteriol. **166:**914–923.
32. **Marchler, G., C. Schüller, G. Adam, and H. Ruis.** 1993. A *Saccharomyces cerevisiae* UAS element controlled by protein kinase A activates transcription in response to a variety of stress conditions. EMBO J. **12:**1997–2003.
33. **Marmorstein, R., M. Carey, M. Ptashne, and S. C. Harrison.** 1992. DNA recognition by GAL4: structure of a protein-DNA complex. Nature **356:**408–414.
34. **Marmorstein, R., and S. C. Harrison.** 1994. Crystal structure of a PPR1-DNA complex: DNA recognition by proteins containing a Zn_2Cys_6 binuclear cluster. Genes Dev. **8:**2504–2512.
35. **Martinez-Pastor, M. T., G. Marchler, C. Schuller, A. Marchler-Bauer, H. Ruis, and F. Estruch.** 1996. The *Saccharomyces cerevisiae* zinc finger proteins Msn2p and Msn4p are required for transcriptional induction through the stress-response element (STRE). EMBO J. **15:**2227–2235.
36. **Matsura, A., M. Treinin, H. Mitsuzawa, Y. Kassir, I. Uno, and G. Simchen.** 1990. The adenylate cyclase/protein kinase cascade regulates entry into meiosis in *Saccharomyces cerevisiae* through the gene *IME1*. EMBO J. **9:**3225–3232.
37. **Miller, J. H.** 1972. Experiments in molecular genetics. Cold Spring Harbor Laboratory Press, Cold Spring Harbor, N.Y.
38. **Misra, V., S. Walker, P. Yang, S. Hayes, and P. O'Hare.** 1996. Conformational alteration of Oct-1 upon DNA binding dictates selectivity in differential interactions with related transcriptional coactivators. Mol. Cell. Biol. **16:**4404–4413.
39. **Mitchell, A. P.** 1994. Control of meiotic gene expression in *Saccharomyces cerevisiae*. Microbiol. Rev. **58:**56–70.
40. **Mitchell, A. P., S. E. Driscoll, and H. E. Smith.** 1990. Positive control of sporulation-specific genes by the *IME1* and *IME2* products in *Saccharomyces cerevisiae*. Mol. Cell. Biol. **10:**2104–2110.
41. **Navas, T. A., Y. Sanchez, and S. J. Elledge.** 1996. *RAD9* and DNA polymerase I form parallel sensory branches for transducing the DNA damage checkpoint signal in *Saccharomyces cerevisiae*. Genes Dev. **10:**2632–2643.
42. **Park, H.-D., R. M. Luche, and T. G. Cooper.** 1992. The yeast *UME6* gene product is required for transcriptional repression mediated by the *CAR1 URS1* repressor binding site. Nucleic Acids Res. **20:**1909–1915.
43. **Perozzi, G., and S. Prakash.** 1986. *RAD7* gene of *Saccharomyces cerevisiae*: transcripts, nucleotide sequence analysis, and functional relationship between *RAD7* and *RAD23* gene product. Mol. Cell. Biol. **6:**1497–1507.
44. **Pfeifer, K., K.-S. Kim, S. Kogan, and L. Guarente.** 1989. Functional dissection and sequence of yeast HAP1 activator. Cell **56:**291–301.

44a. **Prakash, S., and H. Qiu.** Personal communication.

45. **Rubin-Bejerano, I., S. Mandel, K. Robzyk, and Y. Kassir.** 1996. Induction of meiosis in *Saccharomyces cerevisiae* depends on conversion of the transcriptional repressor Ume6 to a positive regulator by its regulated association with the transcriptional activator Ime1. Mol. Cell. Biol. **16:**2518–2526.
46. **Sancar, G. B.** 1985. Sequence of the *Saccharomyces cerevisiae PHR1* gene and homology of the *PHR1* photolyase to *E. coli* photolyase. Nucleic Acids Res. **13:**8231–8246.
47. **Sancar, G. B., R. Ferris, F. W. Smith, and B. Vandeberg.** 1995. Promoter elements of the *PHR1* gene of *Saccharomyces cerevisiae* and their roles in the response to DNA damage. Nucleic Acids Res. **21:**4320–4328.
48. **Sancar, G. B., and F. W. Smith.** 1989. Interactions between yeast photolyase and nucleotide excision repair proteins in *Saccharomyces cerevisiae* and *Escherichia coli*. Mol. Cell. Biol. **9:**4767–4776.
49. **Schmitt, A. P., and K. McEntee.** 1996. Msn2p, a zinc finger DNA-binding protein, is the transcriptional activator of the multistress response in *Saccharomyces cerevisiae*. Proc. Natl. Acad. Sci. USA **93:**5777–5782.
50. **Sebastian, J., B. Kraus, and G. B. Sancar.** 1990. Expression of the yeast *PHR1* gene is induced by DNA-damaging agents. Mol. Cell. Biol. **10:**4630–4637.
51. **Sebastian, J., and G. B. Sancar.** 1991. A damage-responsive DNA binding protein regulates transcription of the yeast DNA repair gene *PHR1*. Proc. Natl. Acad. Sci. USA **88:**11251–11255.
52. **Shiozaki, K., and P. Russell.** 1996. Conjugation, meiosis, and the osmotic stress response are regulated by Spc1 kinase through Atf1 transcription factor in fission yeast. Genes Dev. **10:**2276–2288.
53. **Siede, W., G. W. Robinson, D. Kalainov, T. Malley, and E. C. Friedberg.** 1989. Regulation of the *RAD2* gene of *Saccharomyces cerevisiae*. Mol. Microbiol. **3:**1697–1707.
54. **Sikorski, R. S., and P. Hieter.** 1989. A system for shuttle vectors and yeast host strains designed for efficient manipulation of DNA in *Saccharomyces cerevisiae*. Genetics **122:**19–27.
55. **Singh, K. K., and L. Samson.** 1995. Replication protein A binds to regulatory elements in yeast DNA repair and DNA metabolism genes. Proc. Natl. Acad. Sci. USA **92:**4907–4911.
56. **Skroch, J. M.** 1992. The role of *GAC1* in glycogen metabolism in the yeast *Saccharomyces cerevisiae*. M.S. thesis. North Carolina State University, Raleigh.
57. **Steber, C. M., and R. E. Esposito.** 1995. *UME6* is a central component of a developmental regulatory switch controlling meiosis-specific gene development. Proc. Natl. Acad. Sci. USA **92:**12409–12494.
58. **Strich, R., M. R. Slater, and R. E. Esposito.** 1989. Identification of negative regulatory genes that govern the expression of early meiotic genes in yeast. Proc. Natl. Acad. Sci. USA **86:**10018–10022.
59. **Strich, R., R. T. Surosky, C. Steber, E. Dubois, F. Messenguy, and R. E. Esposito.** 1994. *UME6* is a key regulator of nitrogen repression and meiotic development. Genes Dev. **8:**796–810.
60. **Sun, A., D. S. Fay, and F. Marini.** 1996. Spk1/Rad53 is regulated by Mec1-dependent protein phosphorylation in DNA replication and damage checkpoint pathways. Genes Dev. **10:**395–406.
61. **Szent-Gyorgi, C.** 1995. A bipartite operator interacts with a heat shock element to mediate early meiotic induction of *Saccharomyces cerevisiae HSP82*. Mol. Cell. Biol. **15:**6754–6769.
62. **Takeda, T., T. Toda, K. Kominami, A. Kohnosu, M. Yanagida, and N. Jones.** 1995. *Schizosaccharomyces pombe atf1*$^+$ encodes a transcription factor required for sexual development and entry into stationary phase. EMBO J. **14:**6193–6208.
63. **Tan, S., and T. J. Richmond.** 1990. DNA binding-induced conformational change of the yeast transcriptional activator PRTF. Cell **62:**367–377.
64. **Thompson-Jaeger, S., J. Francois, J. P. Gaughran, and K. Tatchell.** 1991.

Deletion of *SNF1* affects the nutrient response of yeast and resembles mutations which activate the adenylate cyclase pathway. Genetics **129:**697–706.
65. **Unrau, P., R. Wheatcroft, B. S. Cox, and T. Olive.** 1973. The formation of pyrimidine dimers in the DNA of fungi and bacteria. Biochim. Biophys. Acta **312:**626–632.
66. **Vidal, M., A. M. Buckley, C. Yohn, D. J. Hoeppner, and R. F. Gaber.** 1995. Identification of essential nucleotides in an upstream repressing sequence of *Saccharomyces cerevisiae* by selection for increased expression of *TRK2*. Proc. Natl. Acad. Sci. USA **92:**2370–2374.
67. **Werner-Washburne, M., E. Braun, G. C. Johnston, and R. A. Singer.** 1993. Stationary phase in the yeast *Saccharomyces cerevisiae*. Microbiol. Rev. **57:** 383–401.
68. **Xiao, W., K. K. Singh, B. Chen, and L. Samson.** 1993. A common element involved in transcriptional regulation of two DNA alkylation repair genes (*MAG* and *MGT1*) of *Saccharomyces cerevisiae*. Mol. Cell. Biol. **13:**7213–7221.
69. **Yasui, A., and W. Laskowski.** 1975. Determination of the number of photoreactivating enzyme molecules per haploid *Saccharomyces* cell. Int. J. Radiat. Biol. **28:**511–518.
70. **Zhang, L., and L. Guarente.** 1994. The yeast activator HAP1—a GAL4 family member—binds DNA in a directly repeated orientation. Genes Dev. **8:**2110–2119.
71. **Zheng, P., D. S. Fay, J. Burton, H. Xiao, J. L. Pinkham, and D. F. Stern.** 1993. *SPK1* is an essential S-phase-specific gene of *Saccharomyces cerevisiae* that encodes a nuclear serine/threonine/tyrosine kinase. Mol. Cell. Biol. **13:**5829–5842.
72. **Zhou, Z., and S. J. Elledge.** 1993. *DUN1* encodes a protein kinase that controls the DNA damage response in yeast. Cell **75:**1119–1127.